Applied Catalysis A: General 467 (2013) 439–449

Contents lists available at ScienceDirect

Applied Catalysis A: General

journal homepage: www.elsevier.com/locate/apcata

# Flavone complexes of Ti and Zr active in ethylene polymerization

Grasiela Gheno[a], Nara Regina de Souza Basso[b], Marco Antônio Ceschi[a], Paolo R. Livotto[a], Alanjone Azevedo Nascimento[c], Zênis N. da Rocha[c], Griselda Barrera Galland[a,*]

[a] Instituto de Química, Universidade Federal do Rio Grande do Sul, Avenida Bento Gonçalves n° 9500, 91501-970 Porto Alegre, Brazil
[b] Faculdade de Química, Pontifícia Universidade Católica do Rio Grande do Sul, Avenida Ipiranga n° 6681, 90619-900 Porto Alegre, Brazil
[c] Instituto de Química, Universidade Federal da Bahia, Campos de Ondina, 40170-290 Salvador, Bahia, Brazil

ARTICLE INFO

*Article history:*
Received 28 April 2013
Received in revised form 7 August 2013
Accepted 9 August 2013
Available online xxx

*Keywords:*
Synthesis
Complex
3-Hydroxyflavone
Catalyst
Polyethylene

ABSTRACT

Two new complexes of Ti and Zr were synthesized with 3-hydroxyflavone bidentate ligand and investigated in homogeneous ethylene polymerization. Both complexes were characterized by UV–VIS, $^{1}H$ and $^{13}C$ NMR, and electrochemical studies. The geometries and energies of all possible isomeric species were studied by full unconstrained optimizations performed at Density Functional Theory (DFT) level. The polymerization reactions were performed at different experimental conditions with methylaluminoxane (MAO), as the cocatalyst. Both complexes were active in ethylene polymerization in all the conditions used. However, zirconium complex showed the best activity comparing to the titanium complex at 2500 Al/M ratio. The polymers obtained were high density polyethylene with ultra high molecular weights.


## 1. Introduction

The polyolefin production grows, continuously, since the discovery of Phillips and Ziegler–Natta catalysts in the early 1950s [1,2] and this drives the study for new catalysts and new methods for improving the synthesis of these polymers. Polyolefins are cheap and versatile and present good properties that make them widely used in various segments, such as, packaging, building and construction, transportation, medical and health, electrical and electronic devices, agriculture, sport, leisure and design. Global industrial activity in the polyolefin production has reached around 125 millions of tons in 2011 and only in Europe were produced 22 million of tons. More than a half of this total amount was dedicated to manufacturing polyethylenes, including low density polyethylene (LDPE), linear low density polyethylene (LLDPE) and high density polyethylene (HDPE) [3,4].

Intense research has involved the catalysis area and different complexes types for olefin polymerization were investigated, including post-metallocene complexes. Post-metallocene systems can provide some advantages over conventional metallocenes, as for example, the chemical synthesis of complexes can be simpler and more scalable. Some post-metallocene catalysts based on alkoxides bidentate ligands have been proposed in the literature. Sobota synthesized and characterized the crystal structure of the titanium complexes of methylmaltol and guaiacol and verified their catalytic activity in the polymerization of ethylene and propylene [5]. Due to the flexibility of these ligands they easily form complexes with transition metals. Our research group has synthesized various analogs complexes of Ti and Zr based in methylmaltol and ethylmaltol ligands. The synthesized complexes were tested in ethylene polymerization showing activity in homogeneous and heterogeneous conditions [6–9].

The coordination of alcoxide bidentate ligands derivates from flavonoids with transition metal ions has been also investigated. Flavonoids are natural substances of low molecular weight isolated from a wide variety of plants. The basic structure of these compounds consists of 15 carbon atoms arranged into three rings (C6–C3–C6), two substituted phenolic rings (A and B) and a pyrone ring (C) coupled to ring A. The carbon atoms are numbered 2–10 in A and C rings and 1′ to 6′ in B ring [10]. There are several classes of flavonoids differing in the oxidation state and position of hydroxyl and methoxy groups in the two phenyl rings. Most flavonoids contain one or more ortho hydroxy phenolic groups, or one phenolic group with a nearby carbonyl group [11]. Flavonoids are used against various diseases due to their antioxidant activity and pharmaceutical properties as antiinflammatory, antiallergic, anticancer and antimicrobial activities [12]. The 3-hydroxyflavone (3HF) ligand (Fig. 1) has a hydroxyketone functional group present on ring C that is capable of forming complexes with a variety of metals [13]. Several coordination reactions with different metals have been investigated for biomedical purposes, such as complexation of flavonoids with aluminum [13], vanadium [14],

* Corresponding author. Tel.: +55 51 33087317.
*E-mail addresses:* griselda.barrera@ufrgs.br, griselda@iq.ufrgs.br (G.B. Galland).

0926-860X/$ – see front matter © 2013 Elsevier B.V. All rights reserved.
http://dx.doi.org/10.1016/j.apcata.2013.08.015

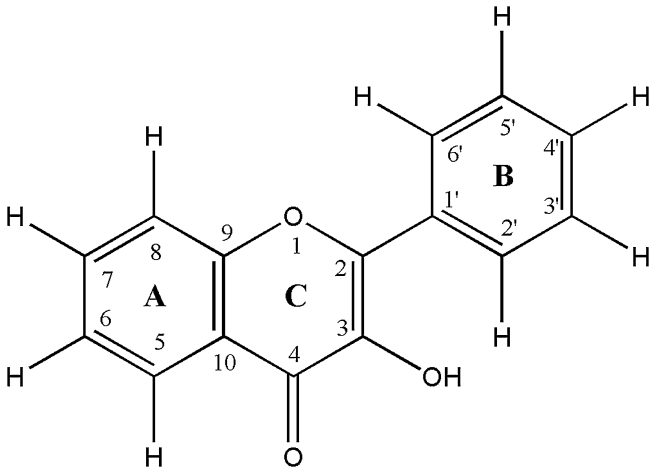


**Fig. 1.** Structure and atomic numbering of 3HF.

nickel (II) [15], iron (III) [16], copper [17], manganese and cobalt [18].

Based on our previous works with the pyrone heterocyclic, we studied the coordination of 3-hydroxyflavone (3HF) bidentate chelating ligand with Ti and Zr and tested the behavior of the two new complexes, dichlorobis(3-hydroxyflavone)titanium(IV) and dichlorobis(3-hydroxyflavone)zirconium(IV) in ethylene polymerization. The advantage in using 3-hydroxyflavone ligand is its provenance from renewable resources and its ease complexation with transition metals. To the best of our knowledge there are not works in the literature reporting those 3-hydroxyflavone-M (M = Ti and Zr) complexes and their activity in ethylene polymerization.

Some parameters such as ethylene pressure, cocatalyst/catalyst ratio and reaction temperature were studied in the aim to improve the catalytic activity.

## 2. Experimental

### 2.1.1. Reagents and materials

All experiments were performed under argon atmosphere using the Schlenk technique. The 3-hydroxyflavone ligand (Aldrich) and $ZrCl_4$ (Merck) were used without purification. All the other reagents used in the present study were of analytical grade. All the solvents were dried by usual methods existing in the literature. MAO (Witco, 10% (w/w) Al in toluene solution) was employed as received. For the Zr complex synthesis it was prepared the $ZrCl_4$·2THF adduct.

### 2.1.2. Synthesis of $ZrCl_4$·2THF adduct

The adduct of $ZrCl_4$ and THF was prepared in a Schlenk under inert atmosphere in the following way: 10 mL of THF was added drop wise, at room temperature, to a stirred suspension of 8.8 g (37.8 mmol) of $ZrCl_4$ in 100 mL of dichloromethane. After 2 h, the pink solution was transferred with a syringe to other Schlenk with a fritted disk. 80 mL of hexane was added to the filtered solution that was filtered again to obtain a white solid that was washed tree times with 10 mL of hexane and dried under vacuum.

### 2.2. Synthesis of the complexes

100 mg of the ligand 3-hydroxyflavone (0.42 mmol) was dissolved in dichloromethane using a Schlenk. Another solution of $MCl_4$ (0.21 mmol, $TiCl_4$ or $ZrCl_4$·2THF) into dichloromethane was drop wise into the solution containing the ligand. The mixture was stirred at room temperature for 1.5 h. Then, the solid was washed twice with diethyl ether, dissolved in dichloromethane and recrystallized in hexane. The complex was dried under vacuum. The dichlorobis(3-hydroxyflavone)titanium(IV), complex 1, brown solid, yield 70%. Elemental analysis: % theoretical calculated for $C_{30}H_{18}O_6TiCl_2$ ($M$ = 592.77 g/mol): C 60.73%, H 3.04%, found: C 60.44%, H 3.08%. $^1$H NMR (300 MHz, $CDCl_3$), $\delta$ (ppm): 8.52 (d, $J$ = 7.4 Hz, 2H, $H_{6',2'}$); 8.08 (d, $J$ = 7.8 Hz, 1H, $H_5$); 7.81 (dd, $J$ = 1.4 and 8.6 Hz, 1H, $H_8$); 7.77 (t, $J$ = 8.7 Hz, 1H, $H_7$); 7.6–7.4 (m, 3H, $H_{3',4',5'}$); 7.42 (t, $J$ = 6.5 Hz, 1H, $H_6$). $^{13}$C NMR (75 MHz, $CDCl_3$), $\delta$ (ppm): 171.4 ($C_4$); 164.9 ($C_9$); 155.6 ($C_2$); 147.1 ($C_3$); 134.9 ($C_7$); 131.9 ($C_{4'}$); 129.7 ($C_{1'}$); 129.3 ($C_{3',5'}$); 129.0 ($C_{2',6'}$); 125.90 ($C_5$); 125.6 ($C_6$); 118.3 ($C_8$); 117.5 ($C_{10}$). The dichlorobis(3-hydroxyflavone)zirconium(IV), complex 2, yellow solid, yield 77%. Elemental analysis: % theoretical calculated for $C_{30}H_{18}O_6ZrCl_2$ ($M$ = 636.12 g/mol): C 56.59%, H 2.83%, found: C 53.03%, H 3.09%. $^1$H NMR (300 MHz, DMSO-$d_6$), $\delta$ (ppm): 8.25 (d, $J$ = 8.3 Hz, 2H, $H_{6',2'}$); 8.16 (d, $J$ = 8.1 Hz, 1H, $H_5$); 7.95 (m, 2H, $H_{7,8}$); 7.65 (td, $J$ = 1.7 and 6.2 Hz, 1H, $H_6$); 7.39 (t, $J$ = 8.4 Hz, 1H, $H_{4'}$); 7.30 (t, $J$ = 6.8 Hz, 2H, $H_{5',3'}$). $^{13}$C NMR (75 MHz, DMSO-$d_6$), $\delta$ (ppm): 179.3 ($C_4$); 154.6 ($C_9$); 148.6 ($C_2$); 146.2 ($C_3$); 134.9 ($C_7$); 130.5 ($C_{1'}$); 130.3 ($C_{4'}$); 128.3 ($C_{3',5'}$); 127.2 ($C_{2',6'}$); 125.9 ($C_5$); 123.7 ($C_6$); 118.8 ($C_{10}$); 117.7 ($C_8$).

### 2.2.1. Complex characterization

The $^1$H NMR spectra of the complexes were recorded on a Varian Inova 300 Spectrometer, using DMSO-$d_6$ or $CDCl_3$ as solvents. The UV–VIS absorption spectra of the ligand and the complex were recorded on a Varian Cary 100 spectrophotometer with quartz cells of 1 cm path length at room temperature. The analyses were performed using acetonitrile as solvent. Elemental analysis (C, H) was performed in a 240 Perkin-Elmer.

### 2.2.2. Theoretical calculations

The geometries and energies of all possible isomeric species were obtained by full unconstrained optimizations performed at Density Functional Theory (DFT) level using the B3LYP hybrid functional obtained by the three parameter fit of the exchange-correlation potential suggested by Becke [19] and the gradient corrected correlation functional of Lee et al. [20]. The polarized Dunning-Huzinaga DZ basis set [21,22] was used for the hydrogen, carbon, chloride and oxygen atoms. For the titanium and zirconium atoms the inner shell electrons were represented by the Los Alamos effective core potential (LANL2) of Hay and Wadt [23,24] and the valence electrons were explicitly included using the associated DZ basis set. All calculations were performed with the Gaussian 03 program using standard procedures and parameters [25].

### 2.2.3. Cyclic voltammetry

The electrochemical measurements, cyclic voltammetry (CV), differential pulse voltammetry (DPV) and electrolysis were taken with a potentiostat EG and G, 273A of Princenton Applied Research. The electronic spectra were obtained with Hewlett-Packard 8453 Spectrometer. All experiments were carried out using a conventional three electrodes cell: glassy carbon was used as working electrode for CV and platinum gauze for electrolysis. An Ag/AgCl electrode was used as the reference electrode and a platinum wire as the auxiliary electrode. Ferrocene (+0.50 V versus Ag/AgCl), was employed as internal standard in acetonitrile solution. A tetrabutylammoniun tetrafluoroborate in acetonitrile solution was used as supporting electrolyte. Successive spectra were recorded during the redox process of the complexes. The supporting electrolyte does not show redox process in the potential range evaluated.

### 2.3. Polymerization reactions

Ethylene polymerizations were performed in a PARR 4843 reactor with 100 mL capacity. Into the reactor was added

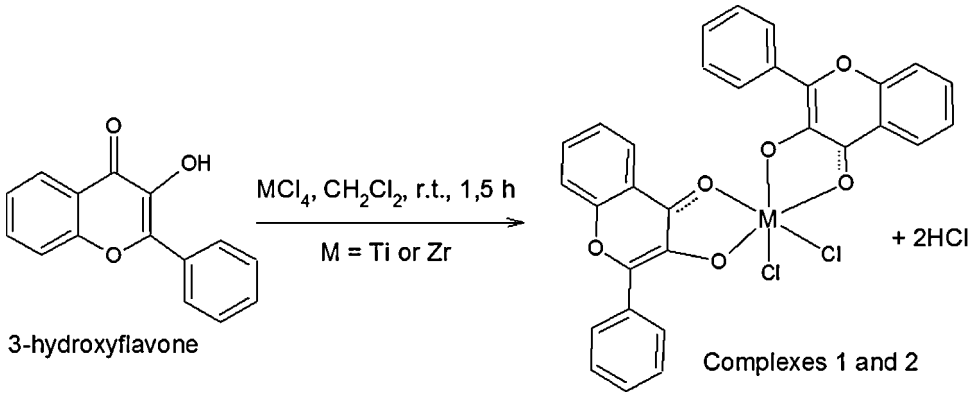


**Scheme 1.** Synthesis of complexes 1 and 2.

30 mL of toluene, methylaluminoxane (MAO) as co-catalyst (co-catalyst/catalyst ratio: 1000, 1500 and 2500) and $10^{-6}$ M of catalyst. The polymerization reactions were performed at 2.8, 4 and 6 bar of ethylene at 40 and 60 °C during 30 min. Acidified ethanol with chloride acid was used to quench the process, and reaction products were separated by filtration, washed with ethanol and acetone, and finally dried.

### 2.3.1. Polymer characterization

The melting points ($T_m$) and crystallinities ($X_c$) of the polymers were determined using a Differential Scanning Calorimeter DSC Q20 TA Instruments with heating of 20–160 °C and heating rate of 10 °C/min with 50 mL/min of $N_2$ flow rate. The heating cycle was performed twice, but only the results of the last scan were considered. The molar masses and molar mass distributions were measured by Gel Permeation Chromatography GPC PL 220 Polymer with RI and VI detector equipped with Water columns (HT6, HT5, HT4, HT3). The mobile phase used was trichlorobenzene (TCB) with 0.1% of BHT at 150 °C at a flow rate of 1 mL/min.

## 3. Results and discussion

The complexes dichlorobis(3-hydroxyflavone)titanium(IV) **(1)** and dichlorobis(3-hydroxyflavone)zirconium(IV) **(2)** were synthesized from 3-hydroxyflavone ligand, as it is shown in Scheme 1.

Fig. 2 shows the $^1$H NMR spectra of 3HF ligand and complex 1. The resonance of the hydroxyl group 3HF ligand at 7.07 ppm disappears in the complex 1 spectrum showing the deprotonation of the 3HF ligand due to the titanium metal insertion. It can be observed in the complex spectrum, the shift of most of the proton signals to higher frequencies in relation to the ligand spectrum, indicating the deshielding effect of the aromatic protons due to the donation of electronic density to the metal. The $^{13}$C chemical shifts of 3HF ligand have already been reported in the literature

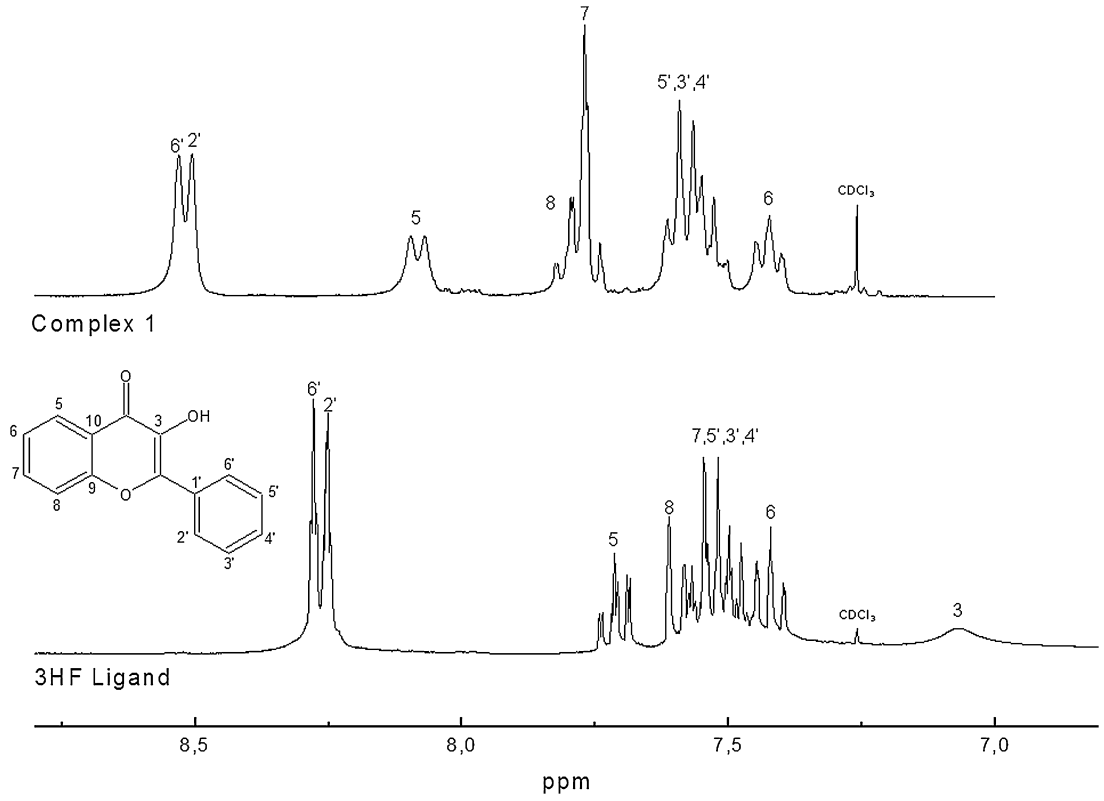


**Fig. 2.** $^1$H NMR spectra of the 3HF ligand and complex 1 in $CDCl_3$.

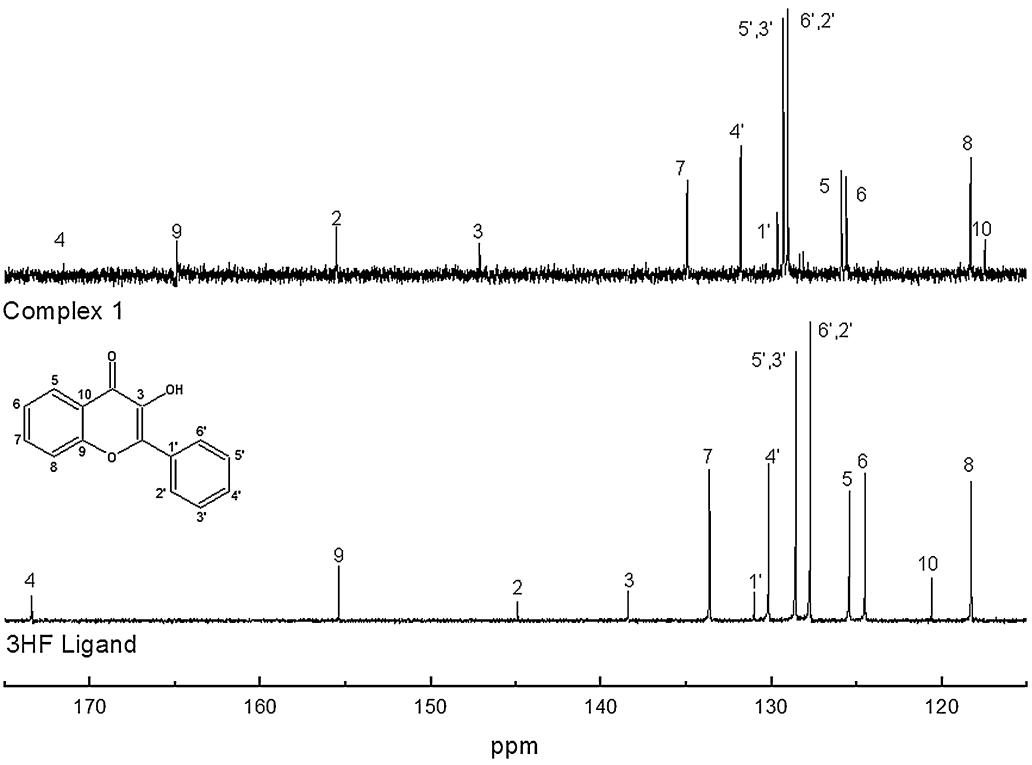


**Fig. 3.** $^{13}C$ NMR spectra of 3HF ligand and complex 1 in $CDCl_3$.

[13,26] and our data is in accordance. Comparing $^{13}C$ NMR spectra of the free ligand and complex 1 at 180–110 ppm region is also observed the displacement of some carbon signals in the complex spectrum, caused by the coordination of the ligand to the metal (Fig. 3).

The $^{1}H$ NMR spectra of 3HF ligand and complex 2 are shown in Fig. 4. The signal at 9.64 ppm in the 3HF ligand spectrum disappears in the complex 2 spectrum showing the deprotonation of hydroxyl group due to the zirconium metal insertion. In addition it was observed the shift of all the protons signals in complex 2

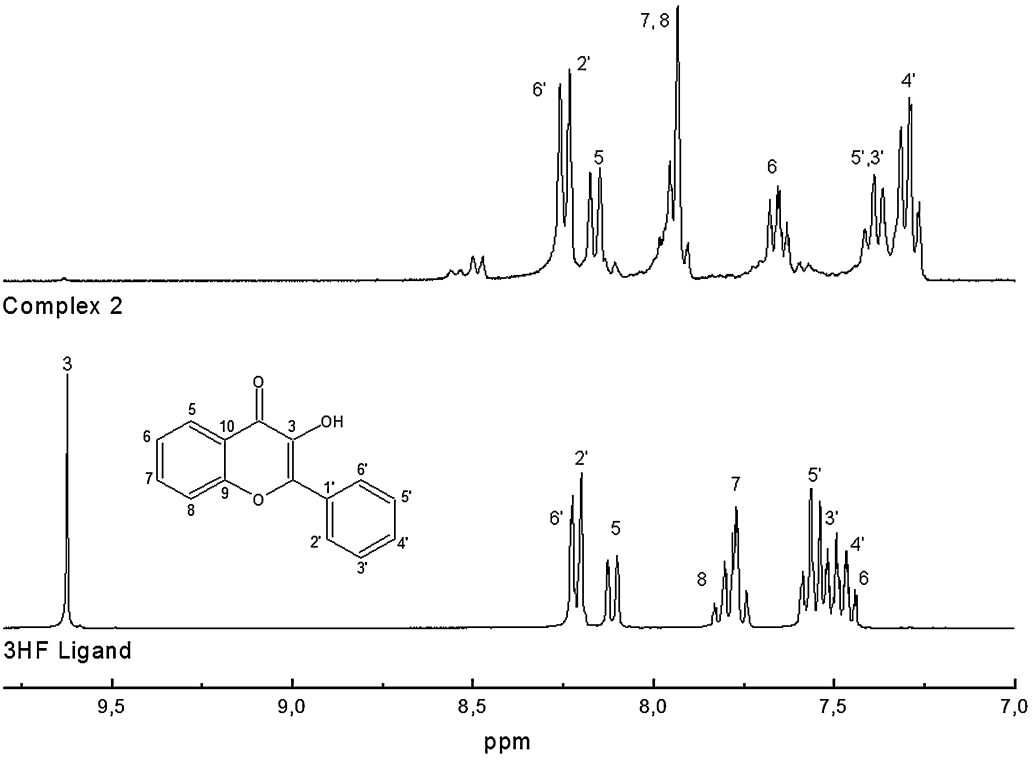


**Fig. 4.** $^{1}H$ NMR spectra of the 3HF ligand and complex 2 in DMSO.

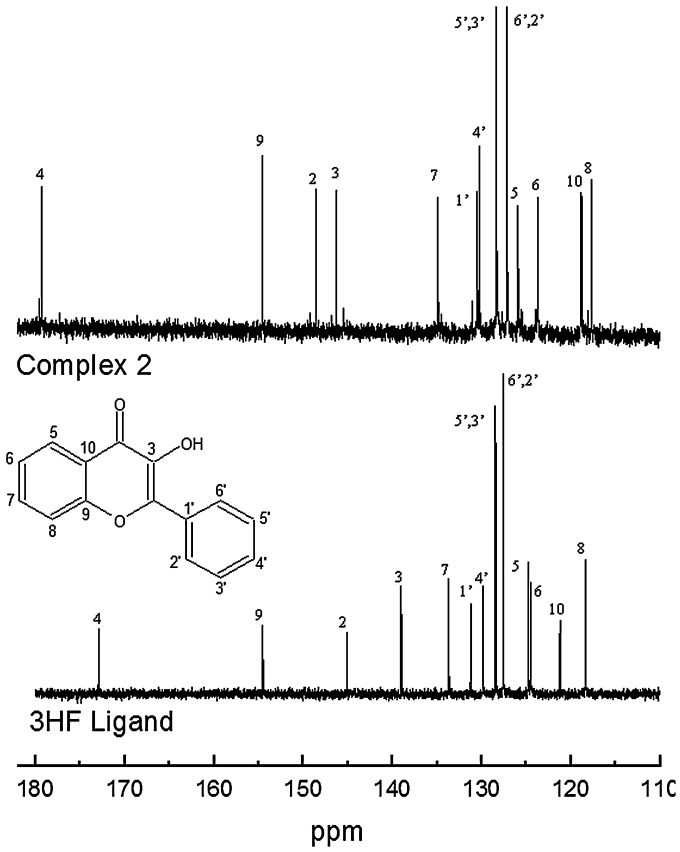


**Fig. 5.** $^{13}$C NMR spectra of 3HF ligand and complex 2 in DMSO.

in relation to the 3HF ligand spectrum. Fig. 5 shows the $^{13}$C NMR expanded spectra of the 3HF ligand and complex 2. In the $^{1}$H NMR spectra of both complexes, it was observed the formation of isomers in small quantities at 8.0 and 7.7 ppm (complex 1) and around 8.5 and 7.8 ppm (complex 2). The hypothesis for the formation of isomers was also justified by the DFT calculations, which shows the possibility of existence of several isomers for each complex synthesized.

The theoretical calculations show that complex 1 can present five isomers, three with *cis* configuration and two with *trans* configuration related to the position of the chlorine atoms. On the other hand, complex 2 can have three *cis* and three *trans* configurations. Fig. 6 shows the structures of these isomers in which the green balls represent chlorine atoms; red balls, oxygen atoms; white balls, hydrogen atoms; ash balls, carbon atoms and the larger balls, the metal (Ti or Zr). The *trans* 2 structure of the complex 1 is not present in Fig. 6 because this structure is unstable and it is unlikely to exist.

Comparing the relative energy and population percentage of all isomers shown in Fig. 6, it is observed that the *cis* structures of both complexes have the lowest relative energy and are therefore more stable than the *trans* structures (Table 1). Among the *cis* configurations, *cis* 2 is the structure of the lowest energy and greatest population percentage for both complexes 1 and 2, therefore the most stable and most likely to exist. This theoretical study is consistent with the results obtained in $^{1}$H NMR spectra of the complexes, which show signs of a main isomer, probably *cis* 2, in greater proportion. Furthermore, the higher possibility of obtaining complexes with *cis* structure is favorable for our purposes because only *cis* isomers are capable of polymerizing ethylene [8].

### 3.1. Electrochemical behavior

The electrochemical behavior of complexes 1 and 2 was investigated by cyclic voltammetry (CV), differential pulse voltammetry (DPV) and controlled potential electrolysis (CPE). Cyclic and pulse voltammograms for uncoordinated 3HF ligand and complexes were recorded in the potential range between 1.8 V and −2.2 V with a scan rate of 100 mV s$^{-1}$ for DPV. The uncoordinated ligand was also studied using CV at scan rates from 0.05 to 0.3 V s$^{-1}$.

Fig. 7 illustrates the DPV with cathodic and anodic scan for the 3HF ligand and complex 1 which demonstrated the reversible of each reduction process. The 3HF ligand shows cathode signals at +1.1, −1.43 and −1.85 V, a shoulder at −1.56 V vs Ag/AgCl (curve a, Fig. 7a). In the anodic scan (curve a, Fig. 7b) there are some signs corresponding to the cathode signals with small displacements due to the existence of a chemical reaction coupled with the redox process.

The existence of chemical reaction coupled to 3HF ligand can be proven by recording the cyclic voltammograms. Fig. 8 (curve a) shows the potential sweep begin at +0.5 V followed by negative potential cathodic signs at −1.50 and −1.90 V and the sweep reverse that illustrates anodic signals at −1.0 and −0.6 V. Moreover, an initial scan at +0.5 V followed by positive potential and further cathodic scan, indicates a lower current intensity of the cathode signals (−1.50 and −1.90 V) and the existence of cathodic signals around −0.1 and −1.0 V (curve b, Fig. 8). In curve b can also be seen a significantly alteration of the current intensities of the anodic signals −1 and −0.6 V and the appearance of an anodic signal at 0.1 V vs Ag/AgCl. Therefore, modification of the curves profile current × potential is indicative that the oxidation and reduction of the 3HF ligand are followed by coupled chemical reaction.

The curves of Fig. 7 show the 3HF ligand cathodic and anodic processes at +1.1 V and shoulder around +0.55 and +0.76 V (anodic scan) vs Ag/AgCl. The complex 1 shows curves of redox processes displaced to more positive values at 1.43 V and shoulders around 0.76 and 1.0 V (anodic scan), which is indicative of the change in electron density in the 3HF ligand when coordinates to the $[TiCl_2]^{2+}$ fragment. The relocation of the relative values of potential to more positive values indicates greater resistance of the ligand to be oxidized. The comparison between the current × potential curves of

**Table 1**
Molecular energies and energies relating to more stable configurations of complexes 1 and 2.

| Isomer | Complex 1 | | | Complex 2 | | |
|---|---|---|---|---|---|---|
| | Energy[a] | Relative energy[b] | Population (%)[c] | Energy[a] | Relative energy[b] | Population (%)[c] |
| *Trans* 1 | −1693.8065209 | 9794 | 0.00 | −1682.3552703 | 8072 | 0.00 |
| *Trans* 2 | – | – | – | −1682.3507412 | 10,914 | 0.00 |
| *Trans* 3 | −1693.8113058 | 6791 | 0.00 | −1682.3594538 | 5447 | 0.01 |
| *Cis* 1 | −1693.8190431 | 1936 | 3.67 | −1682.3656809 | 1539 | 6.92 |
| *Cis* 2 | −1693.8221281 | 0000 | 96.33 | −1682.3681339 | 0000 | 92.98 |
| *Cis* 3 | −1693.8124134 | 6096 | 0.00 | −1682.3616324 | 4079 | 0.09 |

[a] Hartree.
[b] kcal/mol.
[c] At room temperature, 298 K.

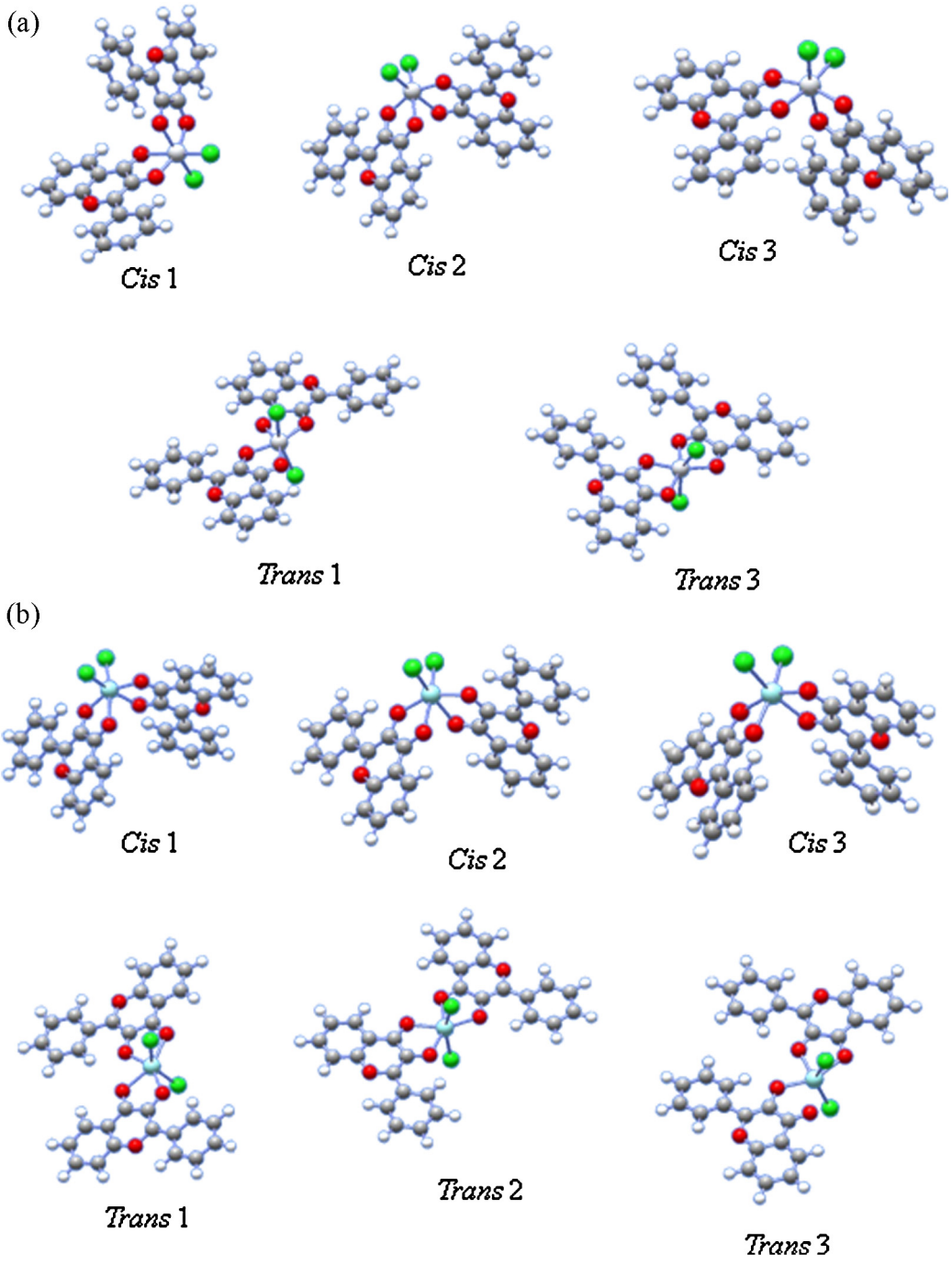


**Fig. 6.** Structures of the possible isomers of (a) complex 1 and (b) complex 2.

the 3HF ligand and complex 1, in the range from 0.0 to −2.0, suggests that the cathodic signals −0.37, −0.81 and −1.22 V vs Ag/AgCl (curve b, Fig. 7a) correspond to redox processes centered on the metallic center, as illustrated in Scheme 2. The proposed electrode process was based on the followed by analogous complexes with pyrone ligands [8,9]. These signals are not present in the DPV profile of 3HF ligand. It was also found that there are shoulders at −1.52 and −1.85 V, which due to the proximity of the uncoordinated ligand signs (curves a, cathodic and anodic sweep) can be assigned to redox processes centered in the coordinated ligand, $L/L^{-}$ and $L^{-}/L^{2-}$.

The profiles of the pulse voltammogram for complex 2 when compared with the free ligand, as occurs for complex 1, illustrated redox process centered at ligand and metallic center. Comparing the curves current vs potential of the Lewis base (3HF ligand), uncoordinated and coordinated to the fragment $[ZrCl_2]$, lead to assign that the cathodic sign of the complex 2 at −0.85 (curve b, Fig. 9a) is a Zr(IV)/III process. Moreover, there are signs at −1.28 and −1.56 in the same curve, which due to the proximity to signals from the uncoordinated ligand can be attributed to redox processes centered in the ligand, $L/L^{-}$ and $L^{-}/L^{2-}$, and also a contribution of redox process centered on the metal center, illustrated in Scheme 2.

Comparing complex 2 with complex 1, it is apparent that the redox processes centered in the ligand on positive potential around 1.2 V and shoulder at 1.6 (cathodic) show no significant change in displacement with the complex 2, the same occurs for redox

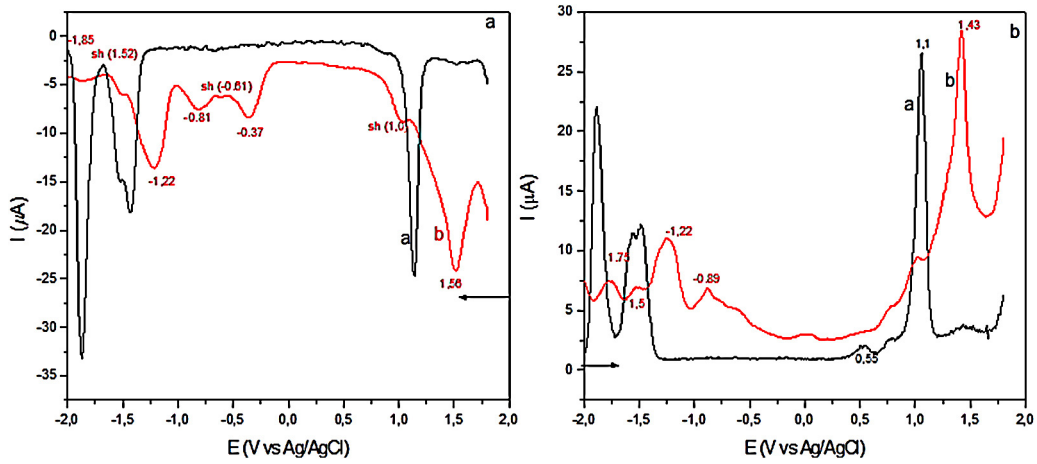


**Fig. 7.** Pulse voltammograms of 3HF ligand (curve a) and complex 1 (curve b): (a) cathodic scan and (b) anodic scan. $\nu = 100\ mV\ s^{-1}$.

$$[M^{IV}Cl_2(3\text{-hydroxyflavone})] \underset{-e^-}{\overset{+e^-}{\rightleftharpoons}} [M^{III}Cl_2(3\text{-hydroxyflavone})]^- \quad \text{(Eq. 1)}$$

$$E_{pc} = -0{,}37\ (Ti) - 1{,}27\ (Zr)$$

$$[M^{III}Cl_2(3\text{-hydroxyflavone})_2]^- \underset{-e^-}{\overset{+e^-}{\rightleftharpoons}} [M^{II}Cl_2(3\text{-hydroxyflavone})_2]^{2-} \quad \text{(Eq. 2)}$$

$$E_{pc} = -0{,}81\ (Ti) - 1{,}43\ (Zr)$$

$$[M^{III}Cl_2(3\text{-hydroxyflavone})_2]^- \rightleftharpoons [M^{III}Cl_2(3\text{-hydroxyflavone})] + 3\text{-hydroxyflavone} \quad \text{(Eq. 3)}$$

$$[M^{III}Cl_2(3\text{-hydroxyflavone})]^- \underset{-e^-}{\overset{+e^-}{\rightleftharpoons}} [M^{II}Cl_2(3\text{-hydroxyflavone})]^{2-} \quad \text{(Eq. 4)}$$

$$E_{pc} = -1{,}22\ (Ti) - 1{,}85\ (Zr)$$

**Scheme 2.** Redox process of the complexes 1 and 2 [$MCl_2$(3HF)] in acetonitrile solution.

negative potentials. These results are indicative of greater binding strength between Ti(IV)-3HF compared to Zr(IV)-3HF, thus leading to greater changes in the electron density of the donor atoms of the coordinated ligand to Ti(IV), therefore there is less tendency for the 3HF ligand to be oxidized.

The results presented for 3HF ligand lead us to propose that the electrode process has a coupled chemical reaction, so for the complexes [$MCl_2$(3HF)] it can be said that they are reversible with a coupled chemical reaction.

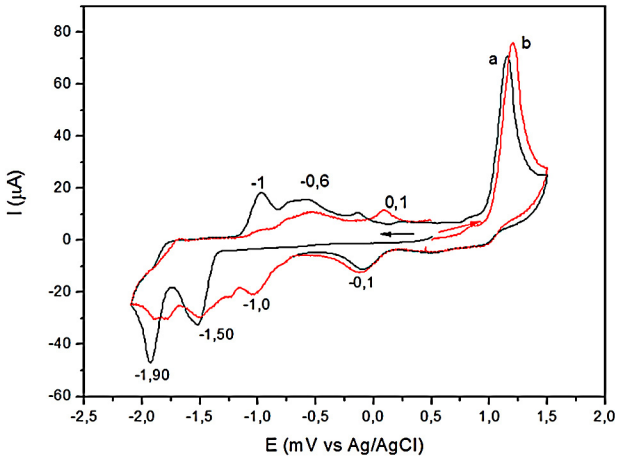


**Fig. 8.** Cyclic voltammograms of 3HF ligand: (a) cathodic scan, (b) anodic scan. $\nu = 100\ mV\ s^{-1}$.

The data indicates that after reduction of Ti(IV) and Zr(IV) there is a labilization of the 3HF ligand, confirmed by the studies of controlled potential electrolysis that support the electrode process proposal shown in Scheme 2. Profiles of the electronic spectra of the original and electrolyzed complexes also appoint to ligand labilization.

Fig. 10 shows the results of controlled potential electrolysis (CPE) at −1.3 V for complex 1 and at −1.4 V vs. Ag/AgCl for complex 2, with appropriate load for engagement of 1, 2 and 3 electrons, which were crucial for confirming the attributed mechanism of electrode. The pulse voltammogram of titanium(IV) complex electrolyzed, with sufficiently load for engaging consumption of ca $1\ F\ mol^{-1}$ (1 electron) illustrated the disappearance of the redox process metal centered at −0.37 V, as shown in Fig. 10a, as a result of chemical reaction subsequent to the reduction of Ti(IV) in the original complex. With the involvement of 3 electrons the profile curve illustrates the existence of cathodic signals corresponding to the reduction of uncoordinated and electrolyzed ligand. For complex 2 analogously to complex Ti(IV) it occurs the disappearance of the cathodic signal at −1.27 V attributed to process Zr(IV)/III, Fig. 10b. Changes in the profile of the curve with the passage of charge up to 3 electrons lead to propose the existence of a coupled chemical reaction.

The electronic spectra of the 3HF ligand and the complexes 1 and 2 are illustrated in Fig. 11. Generally flavonoid compounds have two major absorption bands in the ultraviolet/visible spectra corresponding to the B-ring Band I between 300 and 500 nm (cinnamoyl system) and A-ring, Band II <280 nm (benzoyl system) due to $\pi \rightarrow \pi^*$ electronic transition of an electron from the highest occupied molecular orbital (HOMO) to the lowest unoccupied

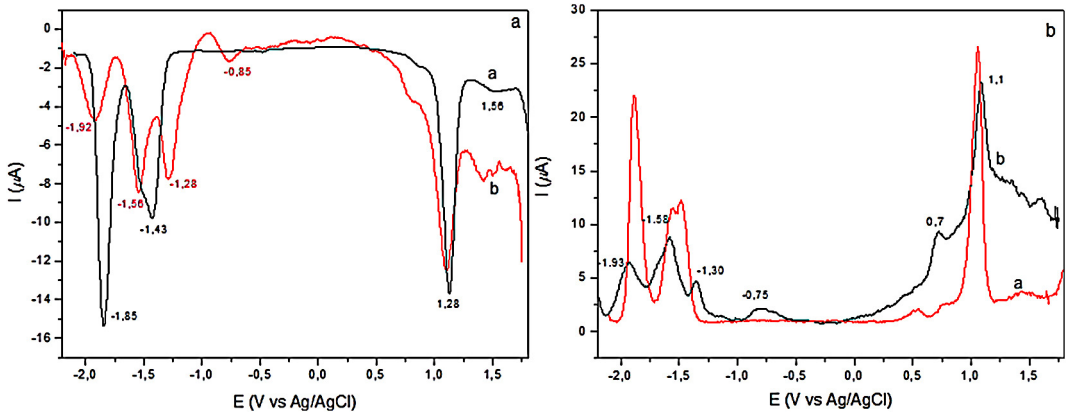


**Fig. 9.** Pulse voltammograms of 3HF ligand (curve a) and complex 2 (curve b): (a) cathodic scan; (b) anodic scan; $\nu = 100\,mV\,s^{-1}$.

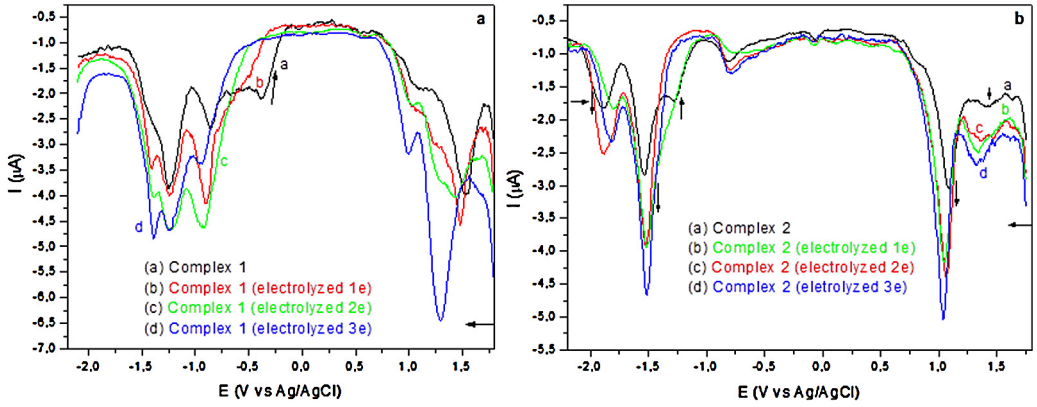


**Fig. 10.** Cyclic voltammogram (a) complex 1 and (b) complex 2: (a) initial; (b) electrolyzed (1 electron); (c) electrolyzed (2 electron); (d) electrolyzed (3 electron). $E$ applied$_{complex1} = -1.3$ V vs Ag/AgCl and $E$ applied$_{complex2} = -1.4$ V vs Ag/AgCl.

molecular orbital (LUMO) as a consequence of conjugation of the double bonds [14,27]. The bands of these systems for 3HF ligand appear at 340 and 300 nm, Band I, and 240 nm, Band II, Fig. 11a. Complex 2 shows another absorption band at 400 nm, probably due to a ligand charge transfer to Zr(IV), absent in the uncoordinated ligand, Fig. 11c.

For the complex 1, Fig. 11b, analogously to the Zr(IV) complex, the spectrum shows an absorption band due to the charge transfer 3HF-Ti(IV). Studies of reduction of the metal center for both complexes show that after the reduction process of Ti the spectrum profile does not change as it occurs in the Zr complex, which is indicative that the Ti(III)-3HF bond strength is stronger than the Zr(III)-3HF, this also explain the smaller tendency of the ligand to output the coordination sphere of the Lewis acid Ti(III).

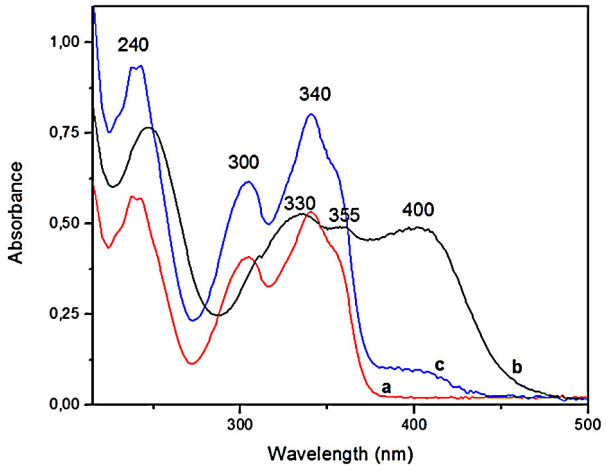


**Fig. 11.** UV–vis spectra in acetonitrile at ambient temperature (a) 3HF ligand, (b) complex 1 and (c) complex 2.

### 3.1.1. *Electrochemical analysis for $[MCl_2(3HF)_2]$ system in the presence of MAO*

The cyclic voltammograms of complexes 1 and 2 in the ethylene and MAO presence were analyzed and illustrated in Fig. 12. The evaluation of the DPV in the ethylene atmosphere compared to the original complex illustrates a small change in the range of −0.8 to −2.0 V, which may result the ethylene coordination. This minor modification shows little influence of the coordination of ethylene to Ti(IV) and Zr(IV) in the electron density of the metal centers. The profiles of the curves recorded after addition of MAO in the solution (curve c, Fig. 12) illustrate the disappearance of the anodic and cathodic waves centered on the metal and assigned to the process M (IV/III). It can be seen in the system containing the complex 1, cathodic signals at −1.55 and −1.9 V and a shoulder in −1.75 V. Analogous, the complex 2 shows cathodic waves at −1.54 and −1.98 V. The potential values in both cases are close to those reported for the 3HF ligand, however in analogy to metallocene Zr(IV) complexes, it can be proposed the abstraction of a chloride by the MAO, leading to the formation of the monomethylated species $[(3HF)_2MCl(Me)]^+$ active in ethylene polymerization [28]. The formation of the active species can also be demonstrated by the existence of activity of both complexes in the ethylene

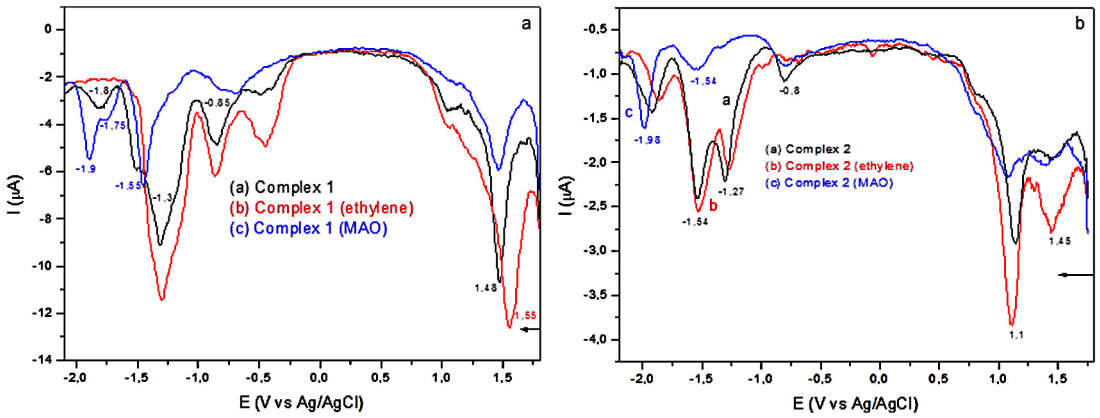


**Fig. 12.** Cyclic voltammogram (a) complex 1 and (b) complex 2: (a) initial; (b) in ethylene atmosphere, (c) in the presence of MAO and in ethylene atmosphere, ratio Al/Ti = 5 and Al/Zr = 2.

polymerization as shown in Table 2. It is worth mentioning that due to the similarity in DPV change when applying a suitable potential for MIV/III reduction (Fig. 10) and the addition of MAO, the possibility of chemical reduction of the metal center cannot be discarded. However, due to the fact that the catalytic systems showed to be active in ethylene polymerization the formation of the methylated species are more probable.

### 3.2. Ethylene polymerization

Catalytic activities of the complexes **1** and **2** were evaluated in homogeneous ethylene polymerization in different experimental conditions. In fact, the effect of Al/M ratio (Al/M = 1000, 1500 and 2500) and ethylene pressure (2.8, 4 and 6 bar) in catalytic activity were studied. The polymerization reactions with complex 1 were performed at 40 °C while the reaction with complex 2 was made at 60 °C. At high temperatures the Zr complexes are more stable and active than complexes based on Ti [8,29]. Table 1 shows the set of evaluated polymerization conditions as well as polymer melting temperature and crystallinity. The complexes showed low and moderate catalytic activity in accordance with literature data for postmetallocene complexes [30]. However, complex 2 presented a quite high catalytic activity when polymerized with a Al/Zr = 2500 and 6 bar of ethylene pressure (entry 18). One of the factors that could explain this difference in catalytic activity between both complexes, it is the difference between oxidation potential of 3HF and reduction potentials of Ti(IV) and Zr(IV), assigned as electrochemical gap ($G$ (V)). The anodic potential for 3HF is around 1.6 V vs Ag/AgCl and cathodic potentials for $Ti^{IV/III}$ and $Zr^{IV/III}$ occur at −0.37 and −1.27 V vs Ag/AgCl, that results in electrochemical values of 1.97 V and 2.87 V, respectively.

Catalyst activity was shown to depend on the complex's metal center and reaction conditions. For titanium complex, the increase in the Al/Ti ratio from 1000 to 1500 increased the catalyst activity in all the different monomer pressures studied, as illustrated in Fig. 13. However the catalytic activity of complex 1 drops dramatically with the increase of the Al/Ti till 2500 at 2.8 and 4 bar of ethylene pressures, remaining constant at 6 bar. This decrease in catalytic activity with increasing Al/Ti ratio may be related to steric hindering caused in the complex due to the excessive amount of MAO used, which can hinder the insertion of ethylene. Studies on Ti complexes of methylmaltol ligand also showed that the catalytic

**Table 2**
Catalytic activity and properties of the homogeneous ethylene polymerization catalyzed by complexes 1 and 2 at different conditions.

| Entry | Complex | Al/M | Ethylene pressure[a] | Activity[b] | $T_m$(°C) | $T_c$(°C) | $X_c$(%) | Mw[c] ×10³ | Mw/Mn |
|---|---|---|---|---|---|---|---|---|---|
| 1 | 1 | 1000 | 2.8 | 18.1 | 136 | 116 | 54 | 1358 | 3.2 |
| 2 | 1 | 1000 | 4 | 10.4 | 135 | 119 | 61 | nd | nd |
| 3 | 1 | 1000 | 6 | 15.6 | 136 | 117 | 61 | nd | nd |
| 4 | 2 | 1000 | 2.8 | 35.5 | 135 | 117 | 52 | nd | nd |
| 5 | 2 | 1000 | 4 | 37.4 | 135 | 118 | 55 | nd | nd |
| 6 | 2 | 1000 | 6 | 49.2 | 136 | 116 | 62 | 636 | 2.3 |
| 7 | 1 | 1500 | 2.8 | 45.6 | 137 | 116 | 45 | 394 | 2.4 |
| 8 | 1 | 1500 | 4 | 24.6 | 135 | 118 | 62 | >3000 | 12.8 |
| 9 | 1 | 1500 | 6 | 30.6 | 136 | 118 | 54 | nd | nd |
| 10 | 2 | 1500 | 2.8 | 31.0 | 135 | 117 | 47 | nd | nd |
| 11 | 2 | 1500 | 4 | 29.1 | 137 | 117 | 56 | nd | nd |
| 12 | 2 | 1500 | 6 | 24.0 | 135 | 118 | 48 | 604 | 2.2 |
| 13 | 1 | 2500 | 2.8 | 4.5 | 134 | 119 | 53 | nd | nd |
| 14 | 1 | 2500 | 4 | 25.4 | 133 | 119 | 18 | nd | nd |
| 15 | 1 | 2500 | 6 | 4.8 | 133 | 119 | 33 | nd | nd |
| 16 | 2 | 2500 | 2.8 | 47.8 | 136 | 116 | 61 | nd | nd |
| 17 | 2 | 2500 | 4 | 36.4 | 136 | 118 | 56 | nd | nd |
| 18 | 2 | 2500 | 6 | 94.2 | 136 | 118 | 52 | 692 | 2.6 |

Reaction conditions: solvent: toluene; time: 30 min; Al: Methylaluminoxane; [M]: $10^{-6}$ mol; temperature: complex 1 at 40 °C and complex 2 at 60 °C. nd: not determined; $\chi_c$: crystallinity.
[a] Bar.
[b] kg/mol h bar.
[c] g/mol.

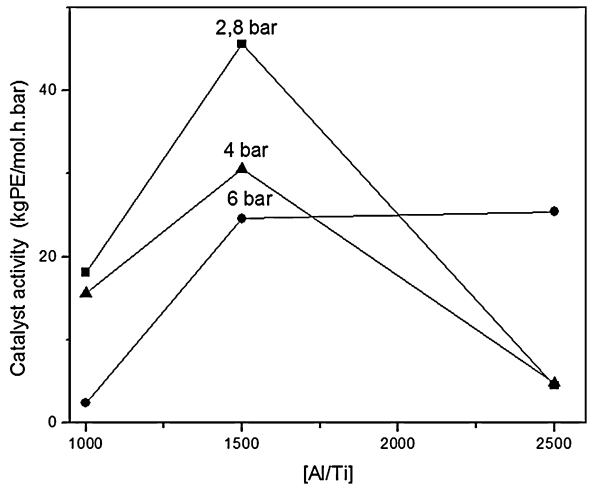


**Fig. 13.** Influence of the Al/Ti molar ratio on the catalyst activity of complex 1.

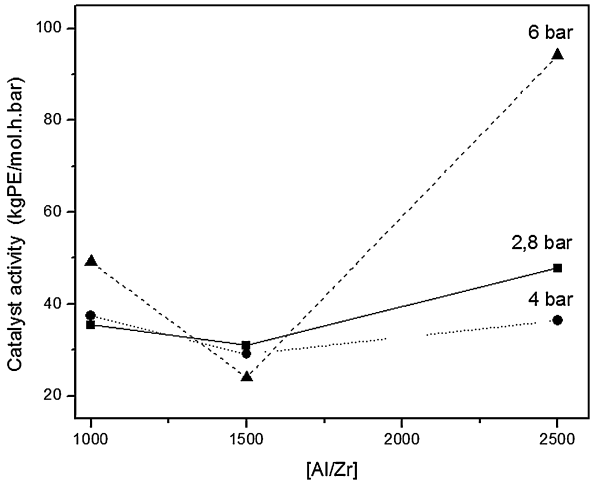


**Fig. 14.** Influence of the Al/Zr molar ratio on the catalyst activity of complex 2.

activity of the Ti complex decreased with increasing Al/Ti ratio and that reduction was attributed to the equilibrium shift in the direction of the ionic pair association between the cationic species and MAO [8]. Moreover, there is also the possibility that the reduction process in the Ti center, observed by voltammetry, generates inactive species for polymerization. However, complex 2 showed a different behavior, in fact, the increase in the Al/Zr ratio from 1000 to 1500 caused a drop in catalytic activity in the three monomer pressures studied. On the other hand, when Al/Zr ratio was increased at 2500, all reactions showed significant increase in catalytic activity, showing that the zirconium complex is more stable at high Al/M ratio (Fig. 14). The polymers obtained with these complexes presented melting temperature between 133 and 137 °C, crystallinity around 52% and ultra high molecular weights. The polydispersity of the polymers were, in general, between 2.2 and 3.2, characteristic of single site catalysts. The polymer obtained in entry 8 had the highest molecular weight >3,000,000 g/mol, and the highest polydispersity, 12.8.

## 4. Conclusions

Two new complexes of titanium and zirconium with the natural origin alkoxide bidentate ligand, 3-hydroxyflavone, were synthesized and characterized by $^{1}H$ and $^{13}C$ NMR, UV–visible, elemental analysis and electrochemical studies. Results from UV–VIS and NMR showed complexation of the ligand to the metal salt, $MCl_4$. NMR spectra also showed the presence of one main isomer. Density Functional Theory confirms the presence of mainly one isomer with the higher probability for the *cis* isomers. The results of the electrochemical study showed that the 3HF ligand is capable of binding to the metal salt due to changes in electron density when it coordinates to the $[MCl_2]^{2+}$ fragment. Studies of reduction of the metal center for both complexes show that after the reduction process of Ti the spectrum profile does not change as it occurs in the Zr complex, which is indicative that the Ti(III)-3HF bond strength is stronger than the Zr(III)-3HF. Furthermore, it was observed that the active species are stabilized in the presence of MAO and also in ethylene atmosphere. Both complexes were active in ethylene polymerization at different reaction conditions. However, the Zr complex showed a better catalytic activity in comparison with the Ti complex, which it could be explained by the different electrochemical behavior.

## Acknowledgements

We thank CAPES, FAPERGS-PRONEX and CNPq for financial support.

## References

[1] H.R. Sailors, J.P. Hogan, J. Macromol. Sci.-Chem. 15 (7) (1981) 1377–1402.
[2] K. Ziegler, E. Holzkamp, H. Breil, H. Martin, Angew. Chem. 57 (1955) 541–547.
[3] Petroleum and Petrochemicals Economics Program: Petrochemical Maerket Dynamics–Polyolefins 2012. http://www.chemsystems.com/reports/search/docs/abstracts/PPE12_PCMD_Polyolefins_Brochure.pdf (accessed at 09.04.13).
[4] Plastics–the Facts 2012. An analysis of European plastics production, demand and waste data for 2011. http://www.plasticseurope.org/Document/plastics-the-facts-2012.aspx?FolID=2 (accessed at 12.04.13).
[5] P. Sobota, K. Przybylak, J. Utko, L.B. Jerzykiewicz, A.J.L. Pombeiro, M.F.C.G. Silva, K. Szczegot, Chem. Eur. J. 7 (2001) 951–958.
[6] C. Carone, V. Lima, F. Albuquerque, P. Nunes, C. Lemos, J.H.Z. Santos, G.B. Galland, F.C. Stedile, S. Einloft, N.R.S. Basso, J. Mol. Catal. A: Chem. 208 (2004) 285–290.
[7] P.P. Greco, R. Brambilla, S. Einloft, F.C. Stedile, G.B. Galland, J.H.Z. Santos, N.R.S. Basso, J. Mol. Catal. A: Chem. 240 (2005) 61–66.
[8] N.R.S. Basso, P.P. Greco, C.L.P. Carone, P.R. Livotto, L.M.T. Simplício, Z.N. Rocha, G.B. Galland, J.H.Z. Santos, J. Mol. Catal. A: Chem. 267 (2007) 129–136.
[9] F.C. Fim, T. Machado, D. Sá, P.R. Livotto, Z.N. Rocha, N.R.S. Basso, G.B. Galland, J. Pol. Sci. A: Pol. Chem. 46 (2008) 3830–3841.
[10] W.C. Dornas, T.T. Oliveira, R.G.R. Dores, A.F. Santos, T.J. Nagem, Rev. Ciênc. Farm. Básica. Apl. 28 (2007) 241–249.
[11] J.P. Cornard, A.C. Boudet, J.C. Merlin, Spectrochim. Acta A 57 (2001) 591–602.
[12] Y. Park, Y.U. Lee, H. Kim, Y. Lee, Y.A. Yoon, B. Moon, Y. Chong, J.H. Ahn, Y.H. Shim, Y. Lim, Bull. Korean Chem. Soc. 27 (2006) 1537–1541.
[13] A.C. Boudet, J.P. Cornard, J.C. Merlin, Spectrochim. Acta A 56 (2000) 829–839.
[14] V. Uivarosi, S.F. Barbuceanu, V. Aldeă, C.C. Arama, M. Badea, R. Olar, D. Marinescu, Molecules 15 (2010) 1578–1589.
[15] J. Tan, L. Zhu, B. Wang, Dalton Trans. (2009) 4722–4728.
[16] G. Baráth, J. Kaizer, G. Speier, L. Párkányi, E. Kuzmann, A. Vértes, Chem. Comm. (2009) 3630–3632.
[17] Q.K. Panhwar, S. Memon, M.I.J. Bhanger, Mol. Struc. 967 (2010) 47–53.
[18] K. Grubel, K. Rudzka, A.M. Arif, K.L. Klotz, J.A. Halfen, L.M. Berreau, Inorg. Chem. 49 (2010) 82–96.
[19] A.D. Becke, Phys. Rev. A 38 (1988) 3098–3100.
[20] C. Lee, W. Yang, R.G. Parr, Phys. Rev. B 37 (1988) 785–789.
[21] T.H. Dunning, P.J. Hay, in: H.F. Schaefer III (Ed.), Modern Theoretical Chemistry 3, Plenum, New York, 1976.
[22] M.J. Frisch, J.A. Pople, J.S. Binkley, J. Chem. Phys. 80 (1984) 3265–3269.
[23] P.J. Hay, W.R. Wadt, J. Chem. Phys. 82 (1985) 270–283.
[24] P.J. Hay, W.R. Wadt, J. Chem. Phys. 82 (1985) 284–298.
[25] Gaussian 03, Revision D., M.J. Frisch, G.W. Trucks, H.B. Schlegel, G.E. Scuseria, M.A. Robb, J.R. Cheeseman, J.A. Montgomery Jr., T. Vreven, K.N. Kudin, J.C. Burant, J.M. Millam, S.S. Iyengar, J. Tomasi, V. Barone, B. Mennucci, M. Cossi, G. Scalmani, N. Rega, G.A. Petersson, H. Nakatsuji, M. Hada, M. Ehara, K. Toyota, R. Fukuda, J. Hasegawa, M. Ishida, T. Nakajima, Y. Honda, O. Kitao, H. Nakai, M. Klene, X. Li, J.E. Knox, H.P. Hratchian, J.B. Cross, V. Bakken, C. Adamo, J. Jaramillo, R. Gomperts, R.E. Stratmann, O. Yazyev, A.J. Austin, R. Cammi, C. Pomelli, J.W. Ochterski, P.Y. Ayala, K. Morokuma, G.A. Voth, P. Salvador, J.J. Dannenberg, V.G. Zakrzewski, S. Dapprich, A.D. Daniels, M.C. Strain, O. Farkas, D.K. Malick, A.D. Rabuck, K. Raghavachari, J.B. Foresman, J.V. Ortiz, Q. Cui, A.G. Baboul,

S. Clifford, J. Cioslowski, B.B. Stefanov, G. Liu, A. Liashenko, P. Piskorz, I. Komaromi, R.L. Martin, D.J. Fox, T. Keith, M.A. Al-Laham, C.Y. Peng, A. Nanayakkara, M. Challacombe, P.M.W. Gill, B. Johnson, W. Chen, M.W. Wong, C. Gonzalez and J.A. Pople, Gaussian, Inc., Wallingford, CT, 2004.
[26] B.H. Moon, Y. Lee, J.H. Ahn, Y. Lim, Magn. Reson. Chem. 43 (2005) 858–860.
[27] A. Torreggiani, M. Tamba, A. Trinchero, S. Bonora, J. Mol. Struct. 744–747 (2005) 759–766.
[28] F. Silveira, L.M.T. Simplício, Z.N. Rocha, J.H.Z. Santos, Appl. Catal. A: Gen. 344 (2008) 98–106.
[29] W. Kaminsky, A. Duch, Catal. Petrol. Ref. Petroch. Ind. (1995) 91–98.
[30] V.C. Gibson, S.K. Spitzmesser, Chem. Rev. 103 (2003) 283–315.